Interim Report IR-99-039

The Dynamics of Invasion Waves

Johan A.J. Metz (metz@rulsfb.leidenuniv.nl)
Denis Mollison (denis@ma.hw.ac.uk)
Frank van den Bosch (frank@rcl.wau.nl)

Approved by

Ulf Dieckmann (dieckman@iiasa.ac.at)
Project Coordinator, Adaptive Dynamics Network

December 1999

Contents

About the Authors

J.A.J. Metz
Section Theoretical Biology
University of Leiden
Leiden, The Netherlands
and
Adaptive Dynamics Network
International Institute for Applied Systems Analysis
A-2361 Laxenburg, Austria

Denis Mollison
Department of Actuarial Mathematics and Statistics
Heriot-Watt University
Edinburgh EH14 4AS, Scotland

Frank van den Bosch
Section Wiskunde
Agricultural University Wageningen
Wageningen, The Netherlands

The Dynamics of Invasion Waves

Johan A.J. Metz
Denis Mollison
Frank van den Bosch

1   Introduction

In this chapter we concentrate on certain macroscopic patterns in the transient behavior of spatially extended ecological systems. Chapters 17 and 22 in Dieckmann et al. 2000 on reaction–diffusion equations also deal with the macroscopic perspective, but from a different angle. Those chapters forego realistic movement and life-history detail in order to concentrate on interactions between individuals. In this chapter, we restrict ourselves to phenomena that are, in general, only weakly dependent on those interactions to arrive at robust and simple quantitative population-level predictions based on measurements of behavioral characteristics of individuals. Luckily, as Chapter 16 in Dieckmann et al. 2000 makes clear, such phenomena are not confined to the realm of mathematics, but commonly occur in real ecological systems as well.

Transient behavior is usually viewed as an effect of a temporary external perturbation of an otherwise stationary situation. From a biological perspective there are two principal types of perturbations. The first type are abiotic perturbations, such as an unusually severe drought; these usually affect large regions, leaving the spatial distributions of species macroscopically homogeneous. The other type of perturbation is the introduction of a new species or the occurrence of an advantageous mutation in an already established species. Such perturbations originate locally and from the initial inoculum spread over space in a wavelike manner. It is the second type of transient behavior that we consider here.

An invasion generally starts with the arrival of a small number of individuals of a new species or a mutation in a single individual. Thus the initial phase of an invasion is dominated by demographic stochasticity. If the invading species survives this phase, it starts to spread from its center of origin until it runs into the boundary of the spatial domain, be it a meadow or a continent. Our main concern is calculating the speed of this spatial spread from life-history data.

Section 2 is devoted to delineating the class of biological systems amenable to our modeling framework. Section 3 contains "do-it-yourself" recipes. Box 1 brings to the fore some special parametric model families with the double virtue that they often efficiently graduate empirical reproductive data and allow efficient numerical calculation of the wave speeds. In Boxes 2 to 4 we consider various special cases for which explicit formulas for the wave speed exist. Box 5 indicates by means of two real-life examples the care that must be taken in matching kernels to field simulations. In Section 4 we discuss the consequences of transgressing the class boundaries. The link with reaction–diffusion models is made in Section 5, where we treat the special conditions under which such models provide useful approximations to our more detailed ones. Finally, Section 6, on stratified dispersal, shows

how the straightforward application of the simple recipes from Section 3 can still lead to unexpected discoveries.

2 Relative Scales of the Process Components

Individual population dynamical behavior has at least four natural length scales set by (1) the dispersal distance; (2) the distance over which the sexes still can attract each other, or over which microgametes (sperm or pollen) are transported; and the distances over which individuals interact ecologically, either (3) directly, by helping each other or fighting, or (4) indirectly, by depleting common resources or boosting local predator densities.

- *Dispersal scale.* With certain provisos (discussed at the end of the next section), the dispersal scale corresponds to the root mean square distance between the birth place of a representative individual and that of its parent. In Section 6 we also consider multiple dispersal mechanisms, each with its own dispersal scale. Treating dispersal as stratified is only necessary when these scales differ by more than one order of magnitude, as is the case for, say, clonal growth and dispersal by seed. In all other sections, we assume that there is only one such mechanism.

- *Sexual scale.* Usually, reproductive output saturates very quickly with increasing mating opportunities. Thus the sexual scale can be defined by the distance between individuals below which offspring production does not suffer from the lack of such opportunities. This distance is infinite for clonally reproducing organisms, self-fertilizers, and organisms that mate before dispersing. From an abstract viewpoint, the spread of a mutant is simply the spread of a clone of the new allele in the genetic and biotic environment set by the resident population. If the sexual attraction distance is short relative to the dispersal distance, individuals in the front of the wave suffer from a lack of mating opportunities. Luckily, sexual attraction distances are often relatively long, so that this effect can be neglected and we can treat the spatial spread of sexual populations in the female-dominant tradition of classical demography.

Although we often can neglect sex during the later phases of an invasion process, we should not forget that an obligately outcrossing population starting from a few individuals has a considerably smaller chance of surviving the initial stochastic phase than a clonal or facultatively self-fertilizing one.

Whereas for our purpose the sexual scale must be large relative to the dispersal scale, exactly the opposite must be true for the ecological interaction scales.

- *Direct interaction scale.* In nature, direct interactions often take place only over distances that are short compared with the dispersal distance. This means that individuals in the front of the dispersing wave have few direct interactions.

- *Indirect interaction scale.* Indirect interactions are more complicated than direct ones. It is possible to dream up scenarios in which predators, feeding on the new invader, increase in numbers beyond proportion and move out from the initial invasion area so quickly as to hamper population increase of the invader at distances far beyond its dispersal distance. Such situations can be treated in the simplified context of reaction–diffusion equations (see, e.g., Hosono 1998), but they fall outside the scope of this chapter. Here, we simply assume that both the direct and indirect interactions act on scales much shorter than the dispersal scale.

In this chapter we confine ourselves to cases without a generalized Allee effect—that is, cases where the ecological interactions between individuals have either no or only detrimental effects on their offspring production at all combinations of age and distance, and females never suffer from a lack of mating opportunities. This restriction allows us to handle relatively realistic life-history patterns.

The requirement to mate is so ubiquitous that we cannot offhandedly dismiss the associated Allee effect. However, it often occurs at such low population densities that its effect on the wave speed should be negligible (see our discussion of the sexual scale above and in Section 4 Interactions).

The assumption that interactions play only a small role in the forward tail of the wave and that any Allee-type effects, whether direct or indirect, are negligible implies that the wave speed is determined only by the linear population dynamics in that forward tail.

A final restriction on the applicability of our framework relates to the scale of any inhomogeneities in the spatio-temporal substrate for the invasion. We proceed as if space and time are homogeneous and infinitely extended, and dispersal is always the same in all directions. In practice, this means that any spatio-temporal inhomogeneities should be either very localized in space compared with the dispersal distance, or have a scale large enough to allow the wave to develop before a region with different properties is reached. In particular, the distance between the location of the inoculum and the boundary of the spatial domain in the direction of the wave movement should be much larger than the dispersal distance, preferably by more than one order of magnitude. When the domain does not have a reflecting boundary, its width in the direction orthogonal to the wave should be considerably larger than the dispersal distance.

A spatially restricted inoculum, rotational symmetry, and translation invariance together lead to asymptotically circular spread at a constant speed (provided no symmetry-breaking destabilization of the wave front occurs; the previous assumptions were rigged to preclude such a destabilization). The next section reviews recipes for calculating this speed for those population systems that comply with the restrictions outlined above. We believe that the simplifying assumptions underlying our calculations are fairly harmless. The most important exceptions occur (1) when the interactions between individuals are already felt at such low densities that there is interference with the demographic stochasticity, and (2) when space is inhomogeneous. In Section 4 we provide some hints as to how those complications may affect the results. We start in the next section with the simple case of individuals that reproduce and disperse independently in a homogeneous space.

3 Independent Spread in Homogeneous Space: A Natural Gauging Point

We have a good grasp of the case of independent spread, down to the level of the full individual-based stochastic process. Biggins (1997) provides a nice survey at a level of biological generality comparable with that of this chapter [with proofs given in Biggins (1995)] and also discusses the intimate relationship between the stochastic and deterministic results. The older deterministic tradition starting with Kolmogorov et al. (1937) and Fisher (1937), followed by Kendall (1957, 1965), Mollison (1972a, 1972b, 1977), who also considers the stochastic case, Atkinson and Reuter (1976), Barbour (1977), Brown and Carr (1977), Aronson and Weinberger (1975), Aronson (1977), Diekmann (1978, 1979), Thieme (1977a, 1977b, 1979a, 1979b), Weinberger (1978, 1982), Radcliffe and Rass (1983, 1984a, 1984b, 1984c, 1984d, 1985, 1986, 1991, 1993, 1995a, 1995b, 1996, 1997, 1998, book in preparation), Lui (1983, 1989a, 1989b), Creegan and Lui (1984), and Kot (1992), im-

mediately took on board some mild forms of nonlinearity. Recent surveys with a focus on applications, and a corresponding stress on the linear deterministic theory, are given by van den Bosch et al. (1990a), Mollison (1991), and Metz and van den Bosch (1995). Here, we also primarily follow the deterministic tradition, since the arguments are easy to convey. In addition, we stick to the case where newborns are stochastically equal—that is, they may differ in some stochastic characteristic, but this characteristic is in no way tied to their parents' birth characteristic or to their space–time coordinates. Analogous results for the case with a Markovian relation between the birth states of parents and offspring can be found in Biggins (1995, 1997), Lui (1983, 1989a, 1989b), and the numerous papers by Radcliffe and Rass cited above.

Model description

Let $b(t, x)$ denote the local birth rate at time t and position x. Then, if the inoculum was put in place at $t = 0-$ and there is no further immigration,

$$
\begin{aligned}
\text{Local birth rate} \quad = \quad &\text{Cumulative local birth rates from} \\
&\text{parents from all places and of all ages,} \\
&\text{born after the moment of inoculation} \\
&\qquad + \\
&\text{Local birth rate from parents in the inoculum ,}
\end{aligned} \tag{1}
$$

or,

$$
b(t, x) = \int_0^t \int_{\mathbb{R}^n} b(t - \tau, x - y) A(\tau, y) \, dy d\tau + h(t, x) , \tag{2}
$$

where n is the dimension of the spatial domain under consideration (in practical applications n = 1, 2, or 3, think of a river bank, a field, or some flask with a protozoan culture in a viscous culture fluid); $A(\tau, y)$ denotes the rate at which a mother aged τ places daughters at a position that is a vectorial distance y from her place of birth; and $h(t, x)$ is the birth rate at x from mothers older than t (i.e., the mothers in the inoculum). In the tradition of the theory of Volterra integral equations, we refer to A as the birth kernel and to h as the initial condition.

As an example, we show how the "reaction"–diffusion model

$$
\frac{\partial n}{\partial t} = D \frac{\partial^2 n}{\partial x^2} + r_0 n \tag{3}
$$

fits into this scheme. The simplest individual-based model giving rise to Equation (3) is one in which individuals diffuse at a rate D, die at rate δ, and give birth in a Poisson process with rate β, so that

$$
r_0 = \beta - \delta . \tag{4}
$$

Under these assumptions, the probability density that an individual survives to age τ and then resides at a position that is distance y from its place of birth is

$$
P(\tau, y) = \exp(-\delta \tau)(4\pi D\tau)^{n/2} \exp[-|y|^2/(4D\tau)] , \tag{5}
$$

and

$$
A(\tau, y) = \beta P(\tau, y) . \tag{6}
$$

For later reference, we introduce the additional terminology

$$R_0 = \int_0^\infty \int_{\mathbb{R}^n} A(\tau, y)\, dy d\tau \;, \tag{7}$$

the average lifetime number of offspring, or reproduction ratio, and, in the case where $R_0 < \infty$,

$$a(\tau, y) = A(\tau, y)/R_0 \;, \tag{8}$$

the birth distribution; we refer to the marginal distributions of the latter as the age-at-birth and displacement distributions. Box 1 in Dieckmann et al. 2000 gives some examples of such distributions that have proved their worth in adapting the theory to practical applications. The mean and variance of the age-at-birth distribution are denoted by μ and ν^2, respectively; the variance of the displacement distribution is denoted by σ^2. For the reaction–diffusion model $R_0 = \beta/\delta$, $\mu = \delta^{-1}$, $\nu^2 = \delta^{-2}$, and $\sigma^2 = 2D/\delta$.

Calculating the wave speed

The various theorems concerning the development of waves are rather intricate. As a first step in our arguments, we consider for $n = 1$ the existence of exponential wave-type solutions, with λ representing the steepness of the wave front,

$$b(t, x) = \alpha \exp[-\lambda(x - ct)] \;, \tag{9}$$

of the time invariant form of Equation (2),

$$b(t, x) = \int_0^\infty \int_{\mathbb{R}} b(t - \tau, x - y) A(\tau, y)\, dy d\tau \;. \tag{10}$$

When we substitute (9) into (10) and rearrange the result, we end up with the characteristic equation

$$L(c, \lambda) = 1 \;, \tag{11}$$

with

$$L(c, \lambda) = \tilde{A}(\lambda c, \lambda) \;, \tag{12}$$

and

$$\tilde{A}(s, \lambda) = \int_0^\infty \int_{-\infty}^\infty \exp(-s\tau - \lambda y) A(\tau, y)\, dy d\tau \tag{13}$$

the Laplace transform of the birth kernel, one-sided in time and two-sided in space.

Using the properties of the Laplace transform, it is easy to show that $L(c, \lambda)$ has the properties depicted in Figure 1. From this we deduce that there exists a c_0 such that Equation (11) allows real solutions for all $c \geq c_0$ and no solutions for $c < c_0$, where c_0 can be calculated from

$$\frac{\partial L}{\partial \lambda}(c_0, \lambda_0) = 0 \;, \qquad L(c_0, \lambda_0) = 1 \;. \tag{14}$$

In practice, c_0 is the only wave speed that matters. To understand why, consider a row of flares, each with a slightly longer fuse than the one preceding it. When the fuses are ignited, a wave of lights progresses at a speed dependent on the differences in the

Box 1 Examples of kernels

To apply the theory from Section 3, we need submodels for the birth kernel. Preferably, such submodels should have a mechanistic basis and (1) be sufficiently flexible when it comes to fitting observed life history data, (2) have a limited number of parameters, and (3) have simple Laplace transforms. Property (3) greatly facilitates solving Equation (14).

In this box, we concentrate on situations where all movement precedes reproduction. This results in birth kernels that can be written as $R_0 a_1(\tau) a_2(y)$, with a_1 being the age-at-birth and a_2 the displacement distribution. The product form is inherited by the Laplace transform. In general, it is expedient to determine R_0 from population observations under the same circumstances as those under which the wave is observed, and a_1 and a_2 from observations of individuals and/or mechanistic submodels.

Age-at-birth distributions. It is rarely possible to find good mechanistic submodels for the age-at-birth distribution. At best we can consider models that do a fair job in the sense of properties (1) to (3) above. A first useful candidate is the block distribution, expressing the assumption that individuals pass through a maturation period of duration p, after which they are fertile at a constant level for a period of duration i. The advantage of block distributions is that the corresponding models can often be rephrased as delay-differential equations. An example is Vanderplank's equation from phytopathology (see Chapter 16 in Dieckmann et al. 2000). The mean and variance are respectively $\mu = p+i/2$ and $\nu^2 = i^2/12$. The Laplace transform is

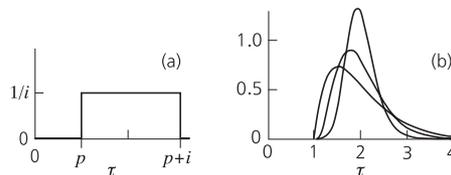$$\tilde{a}_1(s) = \exp(-ps)(is)^{-1}[1 - \exp(-is)] \ .$$

A considerably more flexible family is the delayed gamma densities

$$a_1(\tau) = \begin{cases} 0 & \text{for } 0 < \tau \le p \\ \alpha(\alpha(\tau - p))^{\beta-1} \exp(-\alpha(\tau - p))/\Gamma(\beta) & \text{for } p \le \tau \end{cases}$$

(see Figure 16.13 in Dieckmann et al. 2000), which have mean $\mu = p + \beta/\alpha$, variance $\nu^2 = \beta/\alpha^2$, and Laplace transform

$$\tilde{a}_1(s) = \exp(-ps)[\alpha/(\alpha + s)]^{\beta} \ .$$

Together these two families adequately approximate most age-at-birth distributions.

Some age-at-birth distributions. (a) Block and (b) delayed gamma [with $\beta = 2$ (the lowest peak), 4, 10, and $p = \beta/\alpha = 1$].

Displacement distributions. Formulas purportedly describing displacement distributions abound in the literature. We give three such distributions that we have often found to be good descriptors of empirical data and that moreover can be derived from mechanistic considerations. We gear our discussion to two dimensions, but we only give the Laplace transforms of the one-dimensional marginal distribution used in Equation (14) [see formulas (15) and (17)]. We parameterize with the displacement variance σ^2, which can be estimated by averaging the observed variances in the y_1 and y_2 directions, or, equivalently, as half the observed mean square displacement. Below, "transect distribution" refers to the distribution of offspring over a line transect through the parent. The occupation of home ranges is often well described by a Gaussian distribution. Therefore, a Gaussian is a good descriptor of the transmission of many animal diseases. A Gaussian also results if individuals move for a fixed time according to a (driftless) Brownian motion. Brownian motion is a good description of any continuous movement with little dependence between the displacements in subsequent time intervals, such as in transport by turbulent water or air. The transect and marginal distributions are again Gaussian, with Laplace transform

$$\tilde{a}_2(\lambda, 0) = \exp[(\sigma\lambda)^2] \ .$$

If individuals move for an exponentially distributed time according to a driftless Brownian
continued

Box 1 *continued*

motion, a Bessel distribution results (Broadbent and Kendall, 1953; Williamson, 1961). The transect distribution is

$$a_2(y_1, 0) = \sqrt{2}(\pi\sigma)^{-1}K_0(\sqrt{2}|y_1|/\sigma)$$

[K_0 is the modified Bessel function of the second kind of order zero; see Abramowitz and Stegun (1965)], see Figure 16.14 in Dieckmann et al. 2000. It has variance $\frac{1}{2}\sigma^2$. The marginal distribution is a double exponential one. Its Laplace transform is

$$\tilde{a}_2(\lambda, 0) = [1 - (\sigma\lambda)^2/2]^{-1} .$$

If individuals move for an exponentially distributed time in a straight line, a rotated exponential distribution results. The marginal distribution has Laplace transform

$$\tilde{a}_2(\lambda, 0) = [1 - (\sigma\lambda)^2]^{-1/2} .$$
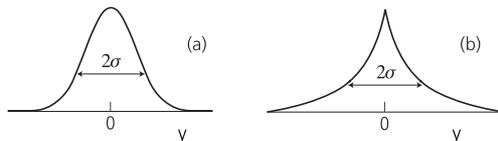
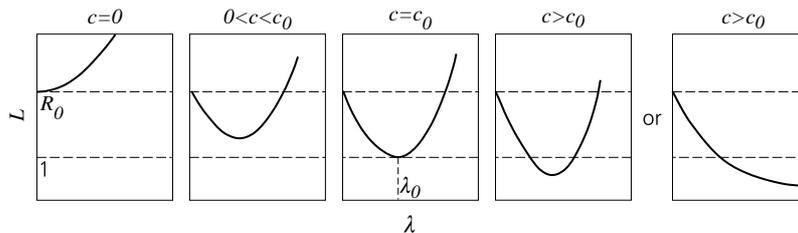Some marginal displacement distributions: (a) Gaussian, (b) double exponential.

Figure 1 Shape of the function L defined by Equations (12) and (13).

lengths of the fuses attached to subsequent flares. However, when the flares can also be ignited by a neighbor, a minimum speed exists. Any slower wave will be overtaken by the autonomous one generated by the mutual ignition. This slowest wave speed is the one that is realized when the process is started up with a localized inoculum.

In general, Equation (14) has to be solved numerically. In the reaction–diffusion case, $c_0 = 2\sqrt{r_0 D} = (\sigma/\mu)\sqrt{2(R_0 - 1)}$. Figure 2 gives contour plots of $c_0^* = \mu c_0/\sigma$ for some other special families of kernels. From these graphs it can be seen that

- for small R_0 the scaled wave speed $c_0^* \approx \sqrt{2\ln R_0}$, with little dependence on either the type of the displacement distribution or the type or the coefficient of variation ν/μ of the age-at-birth distribution;

- for small ν/μ and a Gaussian displacement distribution $c_0^* \approx \sqrt{2\ln R_0}$ for all values of R_0, whereas for small ν/μ and a double exponential displacement distribution $c_0^* \approx \sqrt{1/2}\ln R_0$ for large values of R_0.

These observations form the basis for some useful approximation formulas, discussed in Boxes 2 and 3.
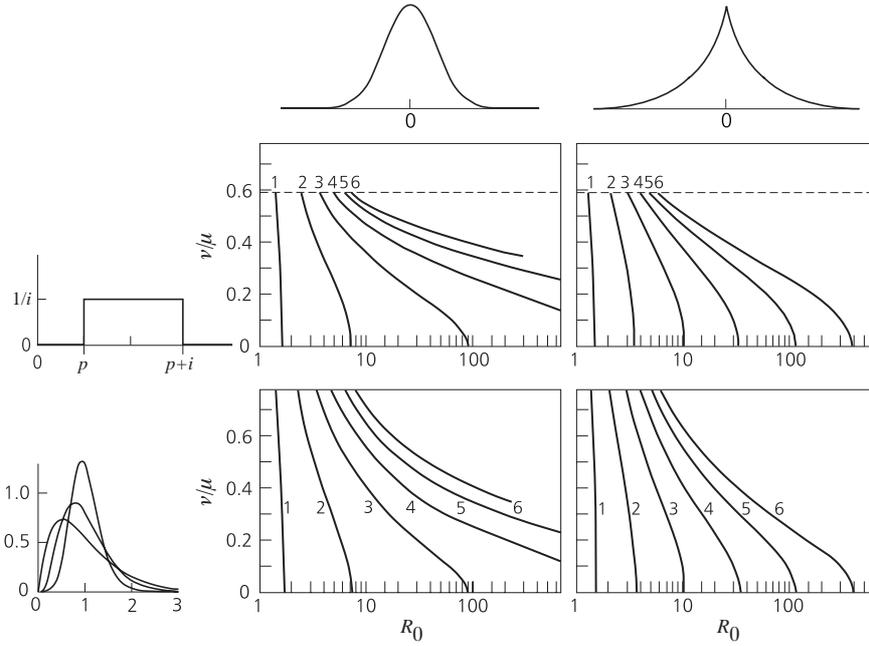
Figure 2 Contour plots of the scaled wave speeds $c_0^* = \mu c_0/\sigma$, for the Gaussian and double exponential displacement distributions, in combination with the block and gamma age-at-birth distributions; μ is the mean age-at-birth; ν is its standard deviation, and σ is the standard deviation of the displacement distribution.

"Run for your life" theorems

The one-dimensional result immediately generalizes to plane or space waves in two and three dimensions, respectively—that is, waves with a profile that is constant in all but one orthogonal direction, for which the speed is measured in the unique remaining direction. All we have to do is replace the birth kernel with the marginal kernel that results from integrating out all but one of the space directions and we are back at the one-dimensional problem. Thus, for $n = 2$ and $y = (y_1, y_2)$, we can calculate the relevant wave speed from Formula (14) together with

$$L(c, \lambda) = \tilde{A}(\lambda c, \lambda, 0) , \tag{15}$$

with

$$\tilde{A}(s, \eta_1, \eta_2) =$$
$$\int_0^\infty \int_{-\infty}^\infty \int_{-\infty}^\infty \exp(-s\tau - \eta_1 y_1 - \eta_2 y_2) A(\tau, y) \, dy_1 dy_2 d\tau , \tag{16}$$

so that

$$\tilde{A}(s, \lambda, 0) = \int_0^\infty \int_{-\infty}^\infty \exp(-s\tau - \lambda y_1) \int_{-\infty}^\infty A(\tau, y) dy_2 \, dy_1 d\tau . \tag{17}$$

Circular or spherical waves are a little more complicated. In an expanding wave the curvature changes. As this curvature necessarily affects the local arrival rate of propagules, we can only expect to see a constant speed emerge after the circle, or sphere, has locally become essentially flat when looked at on the dispersal scale. By the same argument, in combination with those used before, the asymptotic speed of spatial expansion from a localized inoculum should be the same as that of the slowest plane or space waves.

Box 2 Approximation formulas for small $\ln R_0$

In the majority of practical applications $\ln R_0$ is fairly small. For these cases, van den Bosch et al. (1990a) derived the approximative expressions

$$c_0 = \frac{\sigma}{\mu}\sqrt{2\ln R_0}\left\{1 + \left[\left(\frac{\nu}{\mu}\right)^2 - \frac{\kappa_{1,2}}{\sigma^2\mu} + \frac{1}{12}\frac{\kappa_{0,4}}{\sigma^4}\right]\ln R_0 + O\left((\ln R_0)^2\right)\right\},$$

$$\lambda_0 = \frac{1}{\mu}\sqrt{2\ln R_0}\left\{1 - \left[\left(\frac{\nu}{\mu}\right)^2 - 2\frac{\kappa_{1,2}}{\mu\sigma^2} + \frac{1}{4}\frac{\kappa_{0,4}}{\sigma^4}\right]\ln R_0 + O\left((\ln R_0)^2\right)\right\},$$

where the $\kappa_{i,j}$ represent the so-called mixed cumulants of the birth distribution (the first index refers to the age at birth); see, for example, Kendall and Stuart (1958). In the case of rotationally symmetric dispersal (with $\mathbb{E}$ the expectation operator), $\kappa_{1,0} = \mu$, $\kappa_{2,0} = \nu^2$, $\kappa_{0,2} = \sigma^2$, $\kappa_{1,2} = \mathbb{E}\tau y_1^2 - \mu\sigma^2$ (the covariance between the age at birth and the square of the displacement component in a given direction), and $\kappa_{0,4} = \mathbb{E}y_1^4 - 3\sigma^4$. The ratio $\kappa_{0,4}/\sigma^4$ is known as the kurtosis (of the marginal displacement distribution). The following relations are useful for estimation purposes: $\mathbb{E}\tau y_1^2 = \frac{1}{2}\mathbb{E}\tau(y_1^2 + y_2^2)$, $\mathbb{E}y_1^4 = \frac{1}{2}\mathbb{E}(y_1^4 + y_2^4)$. When only prereproductive individuals disperse, $\kappa_{1,2} = 0$. If individuals move unchangingly throughout their lives, $\kappa_{1,2} = \nu^2\sigma^2/\mu$, $\sigma^2 = \mu\acute{\kappa}_2$, $\kappa_{0,4} = \mu\acute{\kappa}_4$, with $\acute{\kappa}_2$ representing the variance and $\acute{\kappa}_4$, the kurtosis of the movement per time unit (see Box 4). The figure shows how well the approximation for c_0 performs for the models of Figure 2.
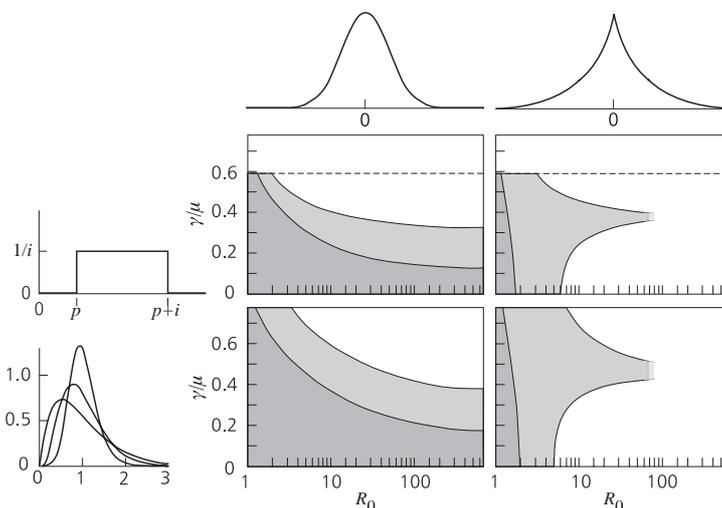
The gray region indicates where the approximation for c_0 differs by less than 10% from the numerical results for the models from Figure 2. The darker gray indicates where the lowest-order term on its own already differs by less than 10%.

Mathematically the convergence to wavelike behavior from some initial condition h is problematic even in the one-dimensional case, both conceptually (What sort of convergence should we think of?) and technically (How should one go about proving it?). Therefore, research has concentrated on the weakest possible form of convergence. Here, we describe the result for $n = 2$. Imagine that you are sitting in a helicopter ascending at speed one, positioned in the sky above $x = 0$. All features on the ground are shrinking in proportion to your altitude. A position x on the ground appears in your field of vision at x/t. Now imagine that every x on the ground for which the local birth rate $b(t, x)$ is between two arbitrary threshold values $b_- < b_+$ is colored black, and every other x is colored white. The black set in your field of vision converges to a circle of radius c_0 around the origin, and everywhere inside that circle the birth rate appears to go to infinity and everywhere outside, to zero. This result is also called the "run for your life" theorem after the following metaphor. Imagine that instead of entering the helicopter you stay on the ground, and that

---

Box 3 Approximations for concentrated reproduction

In this box we give aproximation formulas for the case where reproduction takes place in one very narrow pulse, that is, for small ν/μ. These formulas also can be used to calculate the wave speeds for integro-difference equation models for the spread of a population of annuals (in a seasonal environment) over a continuous spatial domain. If reproduction occurs in a delta peak in time, we can write the birth distribution as a product of that delta peak and the displacement distribution. The Laplace transform of the delta peak at μ is $\tilde{a}_1(s) = \exp(-\mu s)$. We treat only the three diplacement distributions from Box 1. For a Gaussian displacement distribution,

$$c_0 = \frac{\sigma}{\mu}\sqrt{2 \ln R_0} \ .$$

This formula equals the lowest-order term of the formula for c_0 from Box 2. The figure in that box shows how well the approximation predicts the model results.

No explicit formulas are available for the Bessel and rotated exponential distributions. For (very) large R_0 we have the following asymptotic formulas: Bessel: $c_0 \approx \ln R_0/\sqrt{2}$; exponential: $c_0 \approx \ln R_0$. In both cases the R_0 dependence over ranges of one order of magnitude is well described by $c_0 \approx a + b \ln R_0$, even for fairly small R_0 and fairly large ν/μ. This relation was used to good effect by van den Bosch et al. (1990b) in a study of the spread of a fungal pathogen in a wheat field sowed with different mixtures of susceptible and resistant cultivars. The right-hand column of Figure 2 gives an indication how fast a and b change with other model parameters. For $R_0 > 5$ and small ν/μ, the following formulas, with $\rho = \ln R_0$, give values for c_0 that differ by less than 10% from the exact ones:

$$c_0 = \frac{\sigma}{\mu} \frac{2\sqrt{(2\rho + \theta)(2 + \rho)}}{4 - \theta} \ , \quad \theta = \frac{3.2 \ \ln(1 + \rho/2)}{1 + \rho} \quad \text{(Bessel)} \ ,$$

$$c_0 = \frac{\sigma}{\mu} \frac{\sqrt{(\rho + \theta)(1 + \rho)}}{1 - \theta} \quad , \quad \theta = \frac{0.83 \ \ln(1 + \rho)}{1 + 2\rho} \quad \text{(Exponential)} \ .$$

---

you start running in a straight line at speed c. If $c > c_0$ you will outrun the population front, that is, you will see the birth rate dwindle to zero in an exponentially bounded manner. If $c < c_0$, the birth rates in your neighborhood will keep increasing exponentially [i.e., $t^{-1} \ln b(t, ct)$ converges to some constant]. If the movement, survival, and growth of the individuals satisfy some very mild conditions (e.g., postreproductive individuals should not live forever or move faster than reproductive ones, nor should individuals grow at too high an exponential rate), the statements made about the birth rate apply equally to population densities, biomass densities, etc.

More precise forms, as well as proofs, of these rather loose statements can be found in the papers by Diekmann, Thieme, Lui, Radcliffe and Rass, and Biggins, cited at the start of this section.

The "run for your life" theorem has been proved under very general conditions, and it suffices for many practical purposes. But it is also a rather weak result, since it tells nothing about what happens around you when you run at a speed that keeps the birth rate around you more or less constant. Will you see the birth profile around you converge to a constant form? For a few explicitly solvable cases, such as simple diffusion models, one easily obtains the expected result: the profile becomes proportional to $\exp(-\lambda_0 z)$, where z is the distance from your present position and becomes constant in the orthogonal direction. But it is unknown how far this result extends.

In the stochastic case we have to be a little more circumspect. Concepts like the local birth density or the local density of individuals only make sense for means or for deterministic approximations. Our discussion is therefore largely phrased in terms of the numbers

$N(t, r)$ of individuals outside a circle of radius r around the origin (an interval when $n = 1$, a sphere when $n = 3$). If we know $N(t, r)$, we can calculate the number of individuals in a circular band between r_1 and r_2 (where $r_1 < r_2$) by simple subtraction. To get any results, we have to assume that the same innocent conditions needed before to translate results about b into results about numbers of individuals still apply. We only consider the linear case here—that is, we assume that individuals reproduce and disperse independent of each other. In that case, the stochastic mean satisfies the deterministic equations. But, in addition, we have the stronger result that $N(t, ct)$ will almost surely dwindle to zero in an exponentially bounded manner whenever $c > c_0$, and will grow asymptotically like a deterministic exponential, in the sense that $t^{-1} \ln N(t, ct)$ converges to some constant, whenever $c < c_0$. Moreover, the (stochastic) distance $r_{\max}$ of the individual farthest from the origin almost surely satisfies $t^{-1} r_{\max} \to c_0$ (see Biggins 1995, 1997). Again, notwithstanding the beauty and strength of these results, they are in a certain sense rather weak. We look at the data through an ever-more minifying macroscope. The stochastic structure that we may encounter in our immediate surroundings while moving at speed c_0 might be rather subtle. A first hint in this direction can be found in the physics-style results about the asymptotic decomposition of the covariance structure in local and global components presented by Lewis and Pacala (in press).

Spatial scales

The approach followed here is based on the assumption that the integral in Equations (13) and (17) converges for at least some pairs (s, λ). If the far tail of the displacement distribution is so fat that convergence fails, there also is no convergence to a constant wave speed. Instead, in the deterministic case the expanding wave seems to increase ever more in speed (Kot et al. 1996; Clark 1998). And in the stochastic model, any convergence is thwarted by occasional large jumps forward, ruining the development of a deterministic-looking spatial configuration (Mollison 1972b, 1977; Lewis, 1997; Lewis and Pacala, in press). In other words, there is no clear dispersal scale.

In practice, it is nearly impossible to obtain good information about the tails of the displacement distribution. Indeed, there is no far tail because any real system is bounded. What really matters is how well the model under consideration captures the dispersal phenomenon in which we are interested. In that sense, the big jumps forward seen in models with really fat-tailed displacement distributions seem to do a fair job. In Section 5 we discuss another modeling approach to this phenomenon which has the advantage that we can wring some interesting results from it using nothing but Equation (14). Neither approach has yet been shown to be markedly inferior as far as the observations are concerned, and it will be difficult to come to a final verdict (see Appendix 16.A in Dieckmann et al. 2000). The types of models considered in this chapter are by necessity rough approximations to reality, and we are stressing phenomena near the verge of the associated observational resolution. Those interested in the practical aspects are referred to Turchin (1998, Section 6.3 in Dieckmann et al. 2000), and to Clark (1998) and Clark et al. (1998); but see also Appendix 16.A in Dieckmann et al. 2000.

This is also the place to delve a little deeper into the subtleties of the concept of spatial scale. Since the convergence of the integral in Equation (13) is intimately tied to the fact that the tails of the birth kernel are bounded by a negative exponential in the displacement distance (and by some, positive or negative, exponential in time), the relevant dispersal scale in this context is $(\lambda_{\max})^{-1}$, where $\lambda_{\max}$ is the lower bound of those $\lambda > 0$ for which the integral in definition (13) converges. According to our previous discussion, there is no clear dispersal scale if $(\lambda_{\max})^{-1} = \infty$. In Section 1 we identified the dispersal scale with

the root mean square displacement σ of the birthplace of the offspring from that of the mother. This mean square displacement is the appropriate gauge for the dispersal scale when it comes to the scaling of the wave profile λ_0 and speed c_0. Finiteness of $(\lambda_{\max})^{-1}$ implies that σ is finite. For most model families used in practice, the two measures are of the same order of magnitude. Therefore, the precise choice rarely matters, particularly in a heuristic discussion; however, a narrow area of uncertainty remains.

4 Complications

In this section, we briefly consider how the results from the previous section are modified by either spatial and temporal inhomogeneities in the substrate for the invasion, or by interactions between individuals.

Spatial and temporal inhomogeneities, non-isotropy

In practice, our assumption of spatio-temporal homogeneity means that any inhomogeneities should have a very fine spatial grain and be effectively invisible on the dispersal scale. Individuals should be independent; if this is the case, nothing counts but the average of the individual reproductive output over the possible environments in which an individual can find itself, independent of, for example, the temporal scale of the local environmental fluctuations. With temporally fine-grained but spatially widespread inhomogeneities, we have no such luck. Our idealized individuals are assumed to have negligible spatial but considerable temporal extension. Therefore, individuals become effectively independent at a sufficiently fine spatial grain, but remain stochastically dependent when we decrease only the temporal grain.

The heuristic arguments above are supported by analytical results for the diffusion case from Shigesada et al. (1986, 1987). For spatial but no temporal fluctuations, $c_0 \geq 2\sqrt{\langle r_0 \rangle_{\mathrm{A}} \langle D \rangle_{\mathrm{H}}}$, where $\langle \cdot \rangle_{\mathrm{A}}$ denotes the arithmetic and $\langle \cdot \rangle_{\mathrm{H}}$, the harmonic spatial mean, with equality when there are no fluctuations or in the limit of zero environmental grain size. Unfortunately, the figures in Shigesada et al. (1986) show that the speed of convergence to the limit depends rather intricately on the nature of the environmental fluctuations.

Direct calculations for the diffusion case show that for temporal fluctuations alone, $c_0 = 2\sqrt{\langle r_0 \rangle_{\mathrm{A}} \langle D \rangle_{\mathrm{H}}}$, where the averages are now taken in time. In other words, the purely temporal analogue of the spatial limit result is exact.

This last result immediately extends to any model with individuals that diffuse throughout their lives at an age-independent, though time-dependent, rate if we identify $\langle r_0 \rangle_{\mathrm{A}}$ with the overall exponential growth rate of the population. This result is an almost immediate extension of the results in Box 4 in Dieckmann et al. 2000. Unfortunately, there are no easy recipes for determining $\langle r_0 \rangle_{\mathrm{A}}$ from life-history data, except in the special case where the individual birth and death rates depend solely on time, and not on, for example, age. But the result is useful in situations where for other reasons we want to take recourse to a field estimate of $\langle r_0 \rangle_{\mathrm{A}}$ as part of a scheme to estimate the parameters of the birth kernel.

We know from experience that invasion waves may change direction as a result of large-scale spatial inhomogeneities. Therefore, the theory developed in Section 3 is of use only when these inhomogeneities occur on a very large scale, so that the wave has time to relax to its asymptotic speed before the next change in terrain is encountered. Unfortunately, the diffusion theory shows that even the "run for your life" type of convergence only happens at the slow speed of $\ln(t)/t$ (Bramson 1983; Ebert and van Saarloos 1998, unpublished). Some pertinent discussions of the consequences of large-scale spatial inhomogeneity for the

Box 4 Continuous movement

When individuals move in exactly the same manner throughout their lives, the equation for the wave speed can be solved using a two-step procedure.

We first consider the example where individuals move continuously at a constant rate. In that case,

$$A(\tau, y) = B(\tau)(4\pi D\tau)^{n/2} \exp[-|y|^2/(4D\tau)] \ ,$$

where B is the average rate of offspring production at different ages (or R_0 times the age-at-birth distribution), leading to

$$L(c, \lambda) = \tilde{B}(c\lambda - D\lambda^2) = 1 \ ,$$

where $\tilde{B}$ is the Laplace transform of B. A well-mixed population growing according to the same birth regime will, in the long run, grow exponentially at a relative rate r_0 determined by

$$\tilde{B}(r_0) = 1 \ .$$

The combination of Equations (4) and (4) tells us that

$$c\lambda - D\lambda^2 = r_0 \ .$$

The minimum value of c_0 for which this equation still allows a solution for λ can again be found by setting the differentiated left-hand side equal to zero:

$$c_0 = 2D\lambda_0 \ .$$

The combination of the last two equations gives

$$c_0 = 2\sqrt{r_0 D} \ .$$

Thus the square-root formula applies not only to the simple reaction–diffusion case, but also to any model in which individuals diffuse at a constant rate. With a little creative interpretation of the various terms we can also turn this argument on its head: the only non-contrived models that have the same dependence of wave speed on the population-dynamical parameters as reaction–diffusion models assume that individuals diffuse at a constant rate over their entire reproductive lives.

Many observations on real animals suggest that their dispersal is more leptokurtic than purely diffusive. The easiest way to model this is by assuming that they move according to a more general process with independent increments. Biologically, this means that movement rates are highly variable on a very short time scale so that, on the time scale of interest here, movements at different ages are effectively independent. Well-behaved processes of this type can be characterized by the fact that the Laplace transform of the displacement at age τ can be written as $\exp(k(\eta)\tau)$, where k is the so-called infinitesimal cumulant generating function. The coefficients in the Taylor series of k correspond to the cumulants of the distribution of the displacement y at age 1. For such processes,

$$L(c, \lambda) = \tilde{B}(c\lambda - k(\lambda)) \ .$$

[For simplicity, we assume that we are dealing with spread in one dimension, otherwise we have to consider the marginal distribution of k, in the same manner as in Equation (17).] Going through the same motions as before, we find that the wave speed satisfies

$$c_0\lambda_0 - k(\lambda_0) = r_0 \qquad \text{and} \qquad c_0 = k'(\lambda_0) \ .$$

If r is not too large, it suffices to approximate k using estimates for the first terms of its Taylor expansion, which can, for example, be obtained from the estimated cumulants of the dispersal in one direction over one year. If these cumulants are written as $\acute{\kappa}_i$, $\acute{\kappa}_2$ is the variance and $\acute{\kappa}_4$ is the kurtosis (in the diffusion case $\acute{\kappa}_2 = 2D$ and $\acute{\kappa}_4 = 0$),

$$k(\lambda) = \tfrac{1}{2}\acute{\kappa}_2\lambda^2 + \tfrac{1}{24}\acute{\kappa}_4\lambda^4 + \cdots \ .$$

If we stick to the first two terms of the last equation, Equation (14) can be solved explicitly. If the restriction of constant movement applies, the result provides a good approximation for c_0 using only the relatively accessible quantities r_0, $\acute{\kappa}_2$, and $\acute{\kappa}_4$.

analysis of empirical spatial spread patterns can be found in Lubina and Levin (1988) and Andow et al. (1990, 1993). In addition, there is the interesting open theoretical problem of how to transform data about the local values of c_0, derived from life-history data, into statements about changing directions of the wave front (see also Section 8 of Metz and van den Bosch 1995).

In the anisotropic case the linear wave speed changes with the direction of the wave front. The direction-dependent speeds are readily calculated from Equation (14) together with Equations (15) and (16) or (17), with the y_2 direction chosen parallel to the wave front and the y_1 direction, orthogonal to it. The bigger problem is to transform the direction-dependent speed data into a contour that can replace the circle in the "run for your life" theorem. This problem was solved *in abstracto* by Weinberger (1978, 1982) and translated into down-to-earth calculations by van den Bosch et al. (1990a); a more extensive explanation of the recipe can be found in Metz and van den Bosch (1995).

Interactions between individuals

In reality, individuals do not remain independent at ever larger population densities. In the language of deterministic modelers, interactions are equivalent with nonlinearities. Below, we assume that the interactions merely induce a relatively harmless sort of nonlinearity. More particularly, we assume that individuals can never do better reproductively, at any age or distance from their place of birth, than a lonely immigrant just arrived on the scene. We refer to the violation of this assumption as the presence of a generalized Allee effect. However, before we assume that generalized Allee effects are absent, we delve a little deeper into one particular Allee effect that is practically ubiquitous, although mathematically somewhat special.

The Allee effect commonly dealt with in the literature corresponds to an absence of births at low population densities, or at least to such a dearth of births that starting with a uniformly low population density leads to sure extinction. We call this a strict Allee effect, as opposed to the much weaker generalized Allee effect introduced in the previous paragraph. A good discussion of the consequences of a strict Allee effect in the context of reaction–diffusion models can be found in Lewis and Kareiva (1993). Veit and Lewis (1996) analyze a discrete-time model with a strict Allee effect for the spread of the house finch in eastern North America. With a strict Allee effect in place, any waves that arise are pushed by a spillover of individuals from the more crowded regions, whereas in the absence of a generalized Allee effect the waves are pulled by the growth at low population densities in the forward tail of the wave. Because the strict Allee effect "cuts the fuses from our flares," no wave speeds exist other than that corresponding to neighbor ignition. A side effect is that the convergence to the asymptotic wave speed and shape is much faster for pushed waves than for pulled ones. Moreover, a strict Allee effect induces a well-defined asymptotic wave speed even for fat-tailed displacement distributions, since it effectively deactivates any individuals that have moved too far beyond the wave front. The down side is that there is no quick route to calculating the velocity of pushed waves. In principle, all interactions between individuals matter, regardless of whether they come into play at low or at high densities only. However, not all situations are equally dire: the numerical results in Cruickshank et al. (unpublished) show that, at least for some reaction–diffusion models, if a strict Allee effect exists but only plays a role at population densities below those at which the other, detrimental, nonlinearities kick in, we can obtain a good estimate of the wave speed from a linear model in which both types of nonlinearities are ignored. The question is how far this result can be generalized. The displacement kernels corresponding to reaction–diffusion models have about the slimmest tails encountered in

any serious model. We have already seen that any strict Allee effect dramatically alters the conclusions for the fat-tailed case. For exponentially bounded tails, we expect the wave speed to converge to that of the limiting model when the density range over which the Allee effect operates is pushed toward zero, but to converge more slowly for kernels satisfying only weaker exponential bounds.

At this point a warning is in order: generalized Allee effects may spring to life unexpectedly. For example, Hosono (1998) found that the wave speed with which a superior invader takes over in a reaction–diffusion version of the classical Lotka–Volterra competition model is not always equal to $2\sqrt{r_{0i}(1 - \alpha_{ir}K_r)D_i}$, where the indices i and r refer to invader and resident, respectively, α denotes the competition coefficient, and K_r is the equilibrium density of the resident when it is on its own. This result goes directly against the accepted wisdom. The discrepancy arises in cases where the invader so successfully outcompetes the resident that locally the growth rate of the invader can rise well above the depressed value $r_{0i}(1 - \alpha_{ir}K_r)$.

From now on, we assume that Allee effects are absent. This does not necessarily mean that all the effects individuals have on each other are detrimental. It only means that the positive effects can never more than compensate for the detrimental ones if we gauge the results against the situation of an as yet uninvaded environment.

Without an Allee effect, the solution to any deterministic equation for the birth rate is necessarily bounded from above by that of Equation (2), where A is the birth kernel in the uninvaded environment and h is the birth rate from the inoculum as calculated from the full nonlinear model. [For many special models, incorporating the feedback from its fellows into the birth rate of an individual in an equation like Equation (2) is a daunting task. The only advantage of sticking to the integral equation formalism is that this strategy permits some sweeping generalizations.] The wave speed for the nonlinear case is then bounded from above by that of its linearization around the uninvaded state. The fact that the wave speed is determined essentially in the forward tail makes it plausible that the two wave speeds are actually equal, provided that the detrimental effects from higher population densities stay sufficiently localized for the forward tail to be unaffected by the higher population densities further on in the wave. This so-called linear conjecture has been proved for a number of special models (see the references at the start of Section 3). Upon closer inspection, all the apparent exceptions that we know of turn out to violate at least one of the following two assumptions: (1) absence of an Allee effect, or (2) sufficient localization of the interactions. So the linear conjecture forms an excellent first basis for tackling practical problems.

The linear conjecture only refers to the asymptotic speed, and shape, of the far front of the wave. The densities of individuals at any fixed point in space generally increase during the passing of the farthest front. But there is nothing to prevent the initial increase from being followed by crashes as a result of direct or indirect interactions. A second point is that even when the shape of the far front always stabilizes over time, it is not generally true that the population fluctuations in the wake of the wave can be predicted by calculating a unique wave moving at speed c_0. Stabilization of the front does not guarantee the stability of the wake. The difference between the two sorts of stability is demonstrated in the work of Dunbar (1986) and Sherratt et al. (1997) on predator–prey models. Dunbar achieved the mathematical feat of proving the existence of a unique wave with an exponential front and a regularly oscillating rear in a predator–prey model. Ten years later there was a somewhat surprising twist to this result when Sherratt et al. produced numerical simulations indicating that the stable development of the wave front is remarkably robust to even gross changes in the model specification, but that the rear

of the wave is unstable, giving way to irregularly fluctuating spatial patterns. Probably the strongest limitation on the extent of the linear conjecture is found in the work of Bramson (1983) and Ebert and van Saarloos (1998; unpublished), who show that for various reaction–diffusion models there exist asymptotic wave shapes $\hat{b}$ and displacement functions v such that $b(t, z + v(t)) \rightarrow \hat{b}(z)$, with $v(t)/c_0 - t = -\frac{3}{4}\ln(t) + O(1)$ in the nonlinear and $v(t)/c_0 - t = -\frac{1}{4}\ln(t) + O(1)$ in the corresponding linear cases.

So far we have concentrated on deterministic models. However, any deterministic population model ultimately has to be justified by its connection to an underlying individual-based model, which in almost all cases has to be stochastic. The usual route from stochastic to deterministic population models is to assume that population numbers are uniformly large. This assumption cannot hold in the extreme exponential front of a population wave. Those small numbers do not cause a problem because in the front of the wave the individuals are effectively independent. In the independent, or linear, case the association between stochastic and deterministic population models is much stronger, since in that case the deterministic model faithfully represents the mean behavior of the stochastic model at all densities, including arbitrarily low ones. This relation lies at the basis of the strong connection between the stochastic and deterministic "run for your life" results discussed in Section 3. The upshot is that the connection between the stochastic and deterministic results breaks down only when the nonlinearities kick in at densities that are so low that the stochastic effects are not yet negligible.

Nonlinear stochastic "run for your life" results, called "shape theorems" in the stochastic literature, so far have only been proved for models where space is discretized to a square grid. (A good survey can be found in Durrett 1988a, 1988b; see also Cox and Durrett 1988; Zhang 1993.) As yet, no better methods are available for approximating the exact speed than running an efficient simulation of the full spatial stochastic process. Some approximate methods for lattice-based models using a heuristically adapted pair-approximation technique as their main ingredient can be found in Ellner et al. (1998). Lewis (unpublished) has derived adapted moment expansion plus moment closure methods for the continuous-space case by expanding in the size of the neighborhood over which the nonlinear interaction occurs. This procedure has the considerable advantage of allowing the derivation of direct error estimates, but at present the technique remains tied to some very specific assumptions. Overall, both methods perform well in a comparison with simulation results.

Many nonlinear stochastic models can be coupled to a majorating linear model through a thought experiment in which we selectively remove individuals and all their descendants from the output (in mathematical lingo, the sample function) of the linear model in a manner mimicking the stochastic structure of the feedback loop of the nonlinear model (from the population history and/or the present population composition to the death and reproductive events). At all times and places, the population numbers of the linear model are above those of the coupled nonlinear model. This argument proves that the speeds for those nonlinear models are necessarily below that of the associated linear model. Non-Allee nonlinearities only diminish the speed of spatial spread. This effect is clearly demonstrated in Figure 3. The cases considered in this figure are as extreme as possible, since displacement occurs only to the four nearest neighbors on a square grid. For more extended displacement regimes, the speed rapidly converges to that of the associated linear model. Cases where the nonlinearity leads to a speed decrease of more than 50% are rare indeed. However, deviations from the linear results are prominent for the customarily small displacement neighborhoods of grid-based simulations.
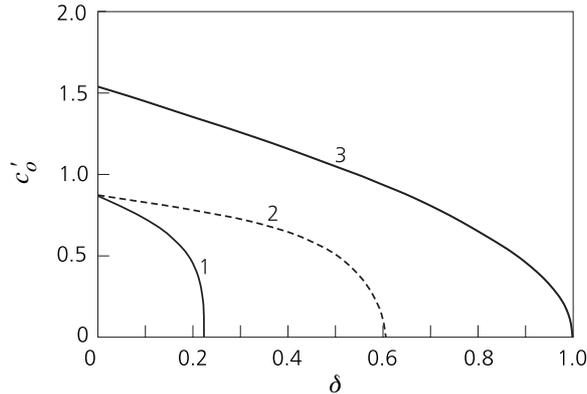
Figure 3 Scaled wave speeds $c_0' = c_0/(\beta\sigma)$ for three nearest-neighbor processes on a square lattice. Individuals are supposed to die at rate δ and give birth at rate β. The offspring are randomly dropped into one of the four nearest cells, so that the displacement variance $\sigma^2 = 1/2$. In the epidemic process (curve 1) offspring dropped into cells that are or have been occupied die. In the contact process (curve 2) only offspring that land in occupied cells die. In the spatial birth and death process (curve 3), the occupation history of a cell has no effect. (The reason for the unusual scaling is that this allows the inclusion of the case $\delta = 0$, for which $\mu = 1/\delta$ is infinite.)

5 The Link with Reaction–Diffusion Models

In Section 3 we discuss one link between our integral-kernel-based models and reaction–diffusion models: the latter can be considered a rather special case of the former. Notwithstanding the somewhat stringent underlying assumptions, reaction–diffusion models often do a good job of capturing the phenomena in which we are interested. Moreover, they are much more accessible mathematically. Reaction–diffusion models are the only models for which results about the convergence to a well-defined wave shape are available, and the numerical calculation of their full solution is relatively easy. The main disadvantage of reaction–diffusion models is their largely phenomenological character. Tying their ingredients to all the wonderful biological detail observable in the field is not always straightforward, or even possible. In this respect, the integral-kernel formalism does a better job.

The main reason reaction–diffusion models do such a good job overall is that they are not just any special case, they are a very special case in that they provide good approximations for large classes of more general models. The remainder of this section contains a heuristic introduction to the inner workings of this approximation.

A first clue about the the way reaction–diffusion models approximate more general population models can be found by comparing our general approximation $c_0 \approx (\sigma/\mu)\sqrt{2\ln R_0}$ for the wave speeds with the speed for the reaction–diffusion model $c_0 = 2\sqrt{r_0 D} = (\sigma/\mu)\sqrt{2(R_0 - 1)}$. This tells us that we can only expect the approximation to work for small R_0. If we also take into account the constraints imposed by their dimensions, we get the following identification of parameters: $r_0 \approx \mu^{-1}\ln R_0 \approx \mu^{-1}(R_0 - 1)$ and $2D \approx \sigma^2/\mu$. (We cheat a little here by already putting the factor 2 in the right place.)

There are two clues for allocating the factor 2. For $R_0 = 1$, the reaction term drops out and we are back to an ordinary diffusion equation. This equation also crops up in the theory of stochastic process as a description of the change over time of a particle undergoing Brownian motion. There, $2D$ corresponds to the variance increment per unit of time. The closest counterpart to such a quantity in our framework is σ^2/μ. The second clue is that the overall exponential growth rate r_0 for general structured populations is well approximated by $\mu^{-1}\ln R_0$ at small values of $\ln R_0$ or ν/μ. So the 2 should not be

allocated to r_0.

Thus we have the connection between the parameters in place for the linear regime. What about any nonlinearities? For the sake of simplicity, we concentrate on nonlinear reaction–diffusion models with direct feedback from the population density to individual behavior

$$\frac{\partial n}{\partial t} = D\frac{\partial^2 n}{\partial x^2} + r(n)n \ . \tag{18}$$

What is the link between the function r and the more complicated underlying population dynamics?

The fuction r has nothing to do with the spatial structure, so for the time being we consider well-mixed populations. The following observations come to mind. The linear considerations told us that we should primarily look at cases where the population density changes only very slowly. We are considering only direct feedback. Therefore, a slowly changing population density means slowly changing circumstances for our individuals. So what guidance can we get from the theory of population growth under constant conditions? In unchanging environments populations will eventually grow exponentially. The relative growth rate can be determined from the nonspatial analogue of Equation (2). Moreover, the population composition stabilizes at an exponential rate, which stays bounded away from zero when we approach the limit of zero growth. If we consider the case of a very small growth rate, we have to rescale time if we still wish to see changes in the population density. In this new time scale, the time in which population structure relaxes to its stable form is very short. The stable form of the population composition is only slightly dependent on the growth rate. In the limit, it is the stable population composition for zero growth rate that, together with the overall population density, enters into the feedback to the reproductive behavior of the individuals. The latter determines the overall population growth rate r. Since the population composition is constant, r effectively only depends on n. Thus we can write $r = \mu^{-1}\ln R(n)$, where $R(n)$ is the average lifetime offspring production of individuals surrounded for their entire lives by conspecifics at a density n in relative frequencies corresponding to the stable population composition (formal details can be found in Greiner et al. 1994, and Metz and van den Bosch 1995).

After this excursion to the general theory of physiologically structured population models, we go a little further into the origin of the diffusion term. In the limit of zero population growth and corresponding constant environment, the basic deterministic equations for our problem become the same as those for a random walk moving to the beat of a renewal process (Cox 1962), because of our assumption that the movement of the individuals is independent across the generations. If we wish to keep the population growth in view, we have to rescale time while taking the limit. The average number of displacement steps made in one time unit by a single line of descent equals μ^{-1}. If we rescale time, this number goes up. Therefore, we have to rescale space to compensate for this increase. However, this combination of time and space scaling is precisely what transforms a random walk into a diffusion (see, e.g., van Kampen 1981).

The upshot is that reaction–diffusion models generically derive from much more general population models through a combination of robust limit procedures. But not every concrete population problem has parameter values putting it close to a reaction–diffusion model!

6 Dispersal on Different Scales

Recently, an increasing number of papers have suggested that dispersal often occurs on two (or more) disparate scales, with most displacement taking place over a fairly short scale, and a small part occurring on a longer scale. The effect of such double dispersal is a wave front consisting of clusters of individuals amid a largely empty space—hence the joy of suddenly discovering a meadow full of a plant species until then only known from some distant country. The down side is that, because long-distance dispersers are few and far between, it is difficult to measure the parameters of the far-dispersal process. Yet it is this dispersal that largely determines the speed of spatial spread. The amplification effect of biological reproduction opens the door to the rare but important events that are the bane of experimental population dynamics (and that, on another time scale, drive evolution).

The combination of a double dispersal mechanism and local population dynamics has two accessible extremes, depending on the interaction of the smallest-scale dispersal and the population dynamical nonlinearity. At the first extreme, the nonlinearity comes into play only late in the passing of the wave front, after the various local clusters have merged into a more or less continuous-looking population. At the other extreme, the local nonlinearities already dominate far out in the wave front. We start with the case where the effect of the nonlinearities stays negligible. A different approach has been taken by Shigesada et al. (1995; see also Shigesada and Kawasaki 1997).

The fully linear case

If the dispersal scales are sufficiently disparate we can concentrate on the larger scale, making the simplifying assumption that all reproduction over the smaller dispersal scale occurs at an individual's place of birth. This leads to reproduction kernels that can be written as the sum of two terms—the term for the far dispersal plus a kernel that is the product of a delta function in space times some time kernel. It turns out that the wave speeds for such models have unexpected properties, which were first brought to light by Cook (unpublished; see also Goldwasser et al. 1994). We demonstrate this phenomenon with the following example.

Imagine a situation in which individuals give birth and die randomly at rates β and δ, respectively, and either stay at home for their whole life with probability p or diffuse at rate D. The birth kernel for this model is, for $n = 1$,

$$
\begin{aligned}
A(\tau, y) = \beta \exp(-\delta\tau)\big[&p\delta_0(y) \\
&+ (1-p)(4\pi D\tau)^{1/2} \exp[-y^2/(4D\tau)]\big] \,,
\end{aligned}
\tag{19}
$$

with δ_0 the delta function at zero. Its Laplace transform is

$$
\tilde{A}(s, \lambda) = \beta[p(s+\delta)^{-1} + (1-p)(s+\delta - D\lambda^2)^{-1}] \,.
\tag{20}
$$

An explicit formula for c_0 cannot be found, but the two equations for λ_0 and c_0 can be reduced to one equation in one unknown, which allows a quick numerical solution. Figure 4 shows the result. Surprisingly, the wave speed does not converge to zero when an increasingly larger fraction of the individuals stay at home. A perturbation expansion gives the following approximate expression for c_0 at small values of p:

$$
c_0 \approx \sqrt{1 - R_0^{-1}} + \sqrt{p(1 + R_0^{-1})} \,.
\tag{21}
$$

What better illustration of the importance of rare events could one wish for?
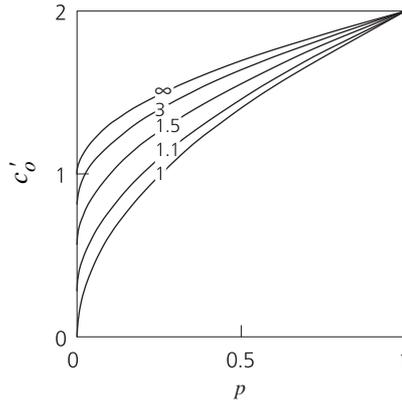
Figure 4 Scaled wave speeds $c_0' = c_0/\sqrt{D(\beta - \delta)}$ for a model in which individuals die at rate δ and give birth at rate β to offspring that either stay at home for their whole life with probability p or diffuse at rate D. (The scaling in this figure differs from the usual scaling since we also want to accommodate the case $\delta = 0$, for which $R_0 = \infty$.) The different curves correspond to the values of $R_0 = \beta/\delta$ indicated on the curve.

Other mixtures of a dispersal kernel and a kernel expressing the fact that some individuals never disperse give the same sort of result. As one more example, consider individuals that reproduce only at age μ and disperse in two dimensions according to the Bessel displacement distribution from Box 1 in Dieckmann et al. 2000 if they disperse at all. Then, $c_0 = (\sigma/\mu)[\ln(R_0)/\sqrt{2} + O(\sqrt{p})]$. The unpleasant message is that, clearly, the rare and therefore difficult to observe far dispersers dominate the picture. The good message is that the customarily low quality of our estimates for the parameter p has less influence on our predictions than we might expect.

When the nonlinearity dominates at the small scale

When new long-distance arrivals are rare and local population growth is fast, we have a situation where the local population dynamical hot-spots (or foci, see Chapter 16 in Dieckmann et al. 2000) develop essentially independent of the large-scale structure of the developing wave. In that case we can treat the hot-spots as individuals in a model that concentrates on the lowest resolution. By concentrating only on the higher resolution we can model the development of the hot-spots as just another nonlinear spatial expansion problem. To simplify the discussion, from now on we assume that $n = 2$. In the simplest case, the local population density inside a hot-spot just grows to a fixed ceiling, so that the output of far dispersers from the hot-spot overall grows like a quadratic function of its age. Another possibility, seen *inter alia* in epidemics, is that the population growth leaves in its wake a burnt-out zone that no longer produces any propagules. In that case the output of far dispersers overall grows like a linear function of age. Although the assumption of a linear or quadratic growth of the output of far dispersers is only a rough approximation, since it does not account for the initial buildup of a hot-spot, we stick to this simplification for the remainder of this section.

The reproduction kernel for the hot-spots can be written as a product of a time kernel, for which we have already chosen $\alpha\tau$ or $\beta\tau^2$, and a displacement distribution. For this we take either the Bessel distribution or the rotated exponential from Box 1 in Dieckmann et al. 2000. The wave speeds for the four possible combinations are as follows:

- Linear $\times$ Bessel: $c_0 = 2^{1/2}\sigma\alpha^{1/2}$

- Linear $\times$ exponential: $c_0 = (27/4)^{1/4}\sigma\alpha^{1/2}$

Box 5 Dependence among parameters: A lesson from rabies

On a number of occasions in this chapter we have broken the birth kernel into components. In this box we wish to introduce a caveat. One should be careful not to let a decomposition that is mathematically convenient guide one's thoughts when it comes to connecting a model to reality. For example, for a fungal disease, sowing a mixture of resistant and susceptible wheat only changes R_0, whereas changing the sowing density changes both R_0 and the dispersal distribution. The following example shows that paying close attention to interpretational matters sometimes allows one to derive interesting conclusions by very modest means.

In 1940 at the Polish–Russian border, a wave of feral rabies began sweeping over Europe. The veterinary and medical importance of rabies has led to considerable modeling effort and the availability of a lot of good data. The primary host for rabies in Europe is the fox. One of the intriguing observations is that the wave speed seems to be largely independent of fox density. When the local fox density is below a certain threshold, rabies does not enter a region at all; in all other cases the wave proceeds at a speed that shows little dependence on fox density (Moegle et al. 1974; Bögel and Moegle 1980). For fox densities above the threshold the earlier models for rabies spread showed a gradual increase in the speed. Van den Bosch et al. (1990a) provided a simple explanation for the discepancy. Although their model is no doubt wrong in its details, the overall message is robust. Transmission of rabies takes place only through direct contact. Foxes have roughly fixed home ranges. Radio-tracking data suggest that home range use by rabid and uninfected foxes does not differ much (Andral et al. 1982). Therefore, we can write $A(\tau, y) = R_0 a_1(\tau) a_2(y)$. It is usual to assume R_0 to be proportional to the local fox density at the start of the epidemic. The argument from Box 1 suggests taking a Gaussian density for a_2. Rabies has a long latent period and a relatively short infectious period. Rough estimates of the mean and standard deviation of the age-at-birth kernel a_1 are respectively $\mu = 35$ days and $\nu = 5$ days (Berger, 1976). The main interest is in the dependence of c_0 on the properties of the local fox community. Lower fox densities correspond both to smaller R_0 and to larger home ranges. More particularly, $\sigma^2 \propto$ [area of home range] $\propto$ [susceptible density]$^{-1} \propto R_0^{-1}$. If we substitute this into the first formula from Box 3, we get

$$c_0 \propto \sqrt{\frac{\ln R_0}{R_0}} \ .$$

To arrive at a quantitative formula, van den Bosch et al. (1990a) used two additional pieces of data gleaned from the literature. At a fox density of 1 fox per km^2, the approximate radius of a home range is 2.3 km (Lambinet et al. 1978), corresponding to $\sigma \approx \sqrt{2.3^2 + 2.3^2} = 3.2$ km, and the observed threshold density for the occurrence of rabies (i.e., $R_0 = 1$) is 0.4 fox per km^2 (Steck and Wandeler 1980). The resulting relation between the predicted speed of the rabies wave and fox densities is depicted in the figure. Effectively, there is either an epidemic wave traveling at a more or less constant velocity, or no epidemic at all. Beyond the threshold density the predicted speed decreases from 45 to 30 km per year for the largest feasible fox densities, which compares well with a reported range of speeds of between 30 and 60 km per year.
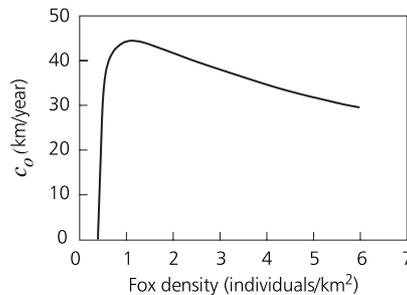
Predicted dependence of speed of rabies spread on fox density.

- Quadratic × Bessel: $c_0 = (5/6)^{1/2} 5^{1/3} \sigma \beta^{1/3}$

- Quadratic × exponential: $c_0 = (4/3)^{1/2} 4^{1/3} \sigma \beta^{1/3}$

On the mathematical side we are in the best possible position. On the empirical side it is a different story. Although we have gone out of our way to produce a parameter-scarce family of models, it is generally impractical to estimate even those few parameters. The theory does, however, provide a basis for organizing comparisons between related species and for studying the potential impact of enforced changes of the parameter values, for example, resulting from a government's agricultural policy. Some initial explorations in the latter direction can be found in van den Bosch et al. (1994, in press); these authors even went so far as to consider disperal on three scales, with the smallest scale dominated by the nonlinearities and the next two scales being treated in the manner outlined in the previous subsection.

7   Concluding Comments

In this section we change the perspective a little and put slightly more emphasis on the inherent stochastic nature of the population processes that underlie the occurrence of invasion waves. Such waves appear when a macroscopically homogeneous system of largish spatial extent is seeded with a concentrated invader mass. By macroscopic spatial homogeneity, we mean that the environment, averaged over the scales at which the individuals interact or disperse, should change little at the spatial scale over which the invasion wave develops. To study the basic properties of invasion waves, we have concentrated on infinitely extended systems. Seen from afar, such waves looks like circles (spheres) extending at an asymptotically constant speed. This speed has been our main object of study. To obtain simple results, we have concentrated on systems without an Allee effect, since for such systems the wave speed is bounded from above by the wave speed of the local linearization around the uninvaded case. However, we have also given arguments for why we expect such systems to be good approximations to systems with a slight strict Allee effect (and no other Allee effect). From the stochastic viewpoint, the main distinction that we have to make is between the locally finite and infinite cases. Systems are effectively locally infinite when the numbers of individuals potentially contained in the dispersal or interaction ranges are sufficiently large and the effect of each separate interaction is correspondingly small. No general quantitative results are available for the locally finite case; all we are able to do is summarize some qualitative trends. The fortunate conclusion is that infinity tends to be rather nearby.

In the locally infinite case, the so-called linear conjecture says that the wave speed of the full model and the wave speed of its local linearization around the uninvaded case coincide. The latter wave speed can be calculated from two equations in two unknowns, expressed in terms of the Laplace transform of the average distribution over time and space of the offspring produced by a single individual. These observations provide the technical background for discussing a number of phenomena, such as the approximation of more complicated population processes by a reaction–diffusion equation, and the curious fact that, in general, the wave speed approaches a nonzero limit when the fraction of individuals who never disperse approaches 1.

References

Abramowitz M, Stegun IA, eds. (1965). *Handbook of Mathematical Functions, with Formulas, Graphs, and Mathematical Tables.* New York, NY, USA: Dover

Andow DA, Kareiva PM, Levin SA, Okubo A (1990). Spread of invading organisms. *Landscape Ecology* 4:177–188

Andow DA, Kareiva PM, Levin SA, Okubo A (1993). Spread of invading organisms: Pattern of spread. In *Evolution of Insect Pests: Patterns of Variation*, ed. Kim KC, McPheron BA, pp. 219–242. New York, NY, USA: Wiley

Andral L, Artois M, Aubert MFA, Blancou J (1982). Radio-pistage de renards enragés. *Comparative Immunology, Microbiology and Infectious Diseases* 5:284–291

Aronson DG (1977). The asymptotic speed of propagation of a simple epidemic. In *Nonlinear Diffusion, Research Notes in Mathematics*, Vol. 14, ed. Fitzgibbon WE, Walker HF, pp. 1–23. London, UK: Pitman

Aronson DG, Weinberger HF (1978). Multidimensional nonlinear diffusion arising in population genetics. *Advances in Mathematics* 30:33–76

Atkinson C, Reuter GE (1976). Deterministic epidemic waves. *Mathematical Proceedings of the Cambridge Philosophical Society* 80:315–330

Barbour AD (1977). The uniqueness of Atkinson's and Reuter's epidemic waves. *Mathematical Proceedings of the Cambridge Philosophical Society* 82:127–130

Berger J (1976). Model of rabies control. In *Mathematical Models in Medicine, Lecture Notes in Biomathematics*, Vol. 11, ed. Berger J, Buhler W, Repges R, Tautu P, pp. 75–88. Berlin: Springer

Biggins JD (1995). The growth and spread of the general branching random walk. *Annals of Applied Probability* 5:1008–1024

Biggins, JD (1997). How fast does a branching random walk spread? In *Classical and Modern Branching Processes*, ed. Athreya KB, Jagers P, pp. 19–39. New York, NY, USA: Springer

Bögel K, Moegle H (1980). Characteristics of the spread of a wildlife rabies epidemic in Europe. *Biogeographica* 8:251–258

Bonde R, Schultz ES (1942/1943). Potato refuse piles as a factor in the dissemination of late blight. *Maine Agricultural Experiment Station Bulletin* 416:229–246

Bourke PMA (1964). Emergence of potato blight, 1843–46. *Nature* 203:805–808

Bramson M (1983). Convergence of solutions of the Kolmogorov equation to travelling waves. *AMS Memoirs*, Vol. 44, No. 285. Providence, RI, USA: American Mathematical Society

Broadbent SR, Kendall DG (1953). The random walk of *Trichostrongylus retortaeformis*. *Biometrics* 9:460–465

Brown KJ, Carr J (1977). Deterministic epidemic waves of critical velocity. *Mathematical Proceedings of the Cambridge Philosophical Society* 81:431–433

Clark JS (1998). Why trees migrate so fast: Confronting theory with dispersal biology and the paleorecord. *The American Naturalist* 15:202–224

Clark JS, Fastie C, Hurt G, Jackson C, Johnson C, King GA, Lewis M, Lynch J, Pacala S, Prentice C, Scupp EG, Webb T III, Wyckoff P (1998). Reid's paradox of rapid plant migration. *Bioscience* 48:13–24

Cook J. Biological Invasions: The Effect of Long-Range Dispersal. Unpublished

Cox DR (1962). *Renewal Theory.* London, UK: Methuen

Creegan P, Lui P (1984). Some remarks about the wave speed and travelling wave solutions of a nonlinear integral operator. *Journal of Mathematical Biology* 20:59–68

Cruickshank I, Gurney WSC, Veitch AR, The characteristics of epidemics and invasions with thresholds. Unpublished

Daniels H (1995). A perturbation approach to nonlinear deterministic epidemic waves. In *Epidemic Models: Their Structure and Relation to Data*, ed. Mollison D, pp. 202–214. Cambridge, UK: Cambridge University Press

Diekmann O (1977). Limiting behaviour in an epidemic model. *Nonlinear Analysis, Theory, Methods and Applications* 1:459–470

Diekmann O (1979). Run for your life. *Journal of Differential Equations* 33:58–73

Dieckmann U, Law R, Metz JAJ, eds. (2000). *The Geometry of Ecological Interactions: Simplifying*

Spatial Complexity. Cambridge, UK: Cambridge University Press

Dunbar SR (1986). Traveling waves in diffusive predatory–prey equations: Periodic orbits and point-to-periodic heteroclinic orbits. *SIAM Journal of Applied Mathematics* 46:1057–1078

Durrett R (1988b). *Lecture Notes on Particle Systems and Percolation*. Pacific Grove, CA, USA: Wadsworth and Brooks/Cole

Ebert U, van Saarloos W (1998). Universal algebraic relaxation of fronts propagating into an unstable state and implications for moving boundary approximations. *Physics Review Letters* 80:2350–2353

Ebert U, van Saarloos W. Fronts propagating uniformly into unstable states: Universal algebraic rate of convergence of pulled fronts. Unpublished

Ellner SP, Sasaki A, Haraguchi Y, Matsuda H (1998). Speed of invasion in lattice population models: Pair-edge approximation. *Journal of Mathematical Biology* 36(5):469–484

Fisher R (1937). The wave of advance of advantageous genes. *Annals of Eugenics* 7:353–369

Goldwasser L, Cook J, Silverman ED (1994). The effects of variability on metapopulation dynamics and rates of invasion. *Ecology* 75:40–47

Greiner G, Heesterbeek J, Metz J (1994). A singular perturbation theorem for evolution equations and time-scale arguments for structured population models. *Canadian Applied Mathematics Quarterly* 2:435–459

Hosono Y (1998). The minimal speed of traveling fronts for a diffusive Lotka–Volterra competition model. *Bulletin of Mathematical Biology* 60:435–448

Kendall DG (1957). In discussion on Bartlett, MS: Measles periodicity and community size. *Journal of the Royal Statistical Society A* 120:48–70

Kendall DG (1965). Mathematical models of the spread of infection. In *Mathematics and Computer Science in Biology and Medicine*, pp. 213–225. London, UK: HMSO

Kendall MG, Stuart A (1958). *The Advanced Theory of Statistics*, Vol. 1. London, UK: Griffin

Kolmogorov A, Petrovsky N, Piskounov NS (1937). A study of the equation of diffusion with increase in the quantity of matter, and its application to a biological problem. *Moscow University Bulletin of Mathematics* 1:1–25

Kot M (1992). Discrete-time travelling waves: Ecological examples. *Journal of Mathematical Biology* 30:413–436

Kot M, Lewis MA, van den Driesche P (1996). Dispersal data and the spread of invading organisms. *Ecology* 77:2027–2042

Lambinet D, Boisvieux JF, Mallet A, Artois M, Andral L (1978). Modèle mathématique de la propagation d'une épizootie de rage vulpine. *Revue d'Epidémiologie et de Santé Publique* 26:9–28

Lewis MA. Spread rate for a nonlinear stochastic invasion. Unpublished

Lewis MA, Kareiva P (1993). Allee dynamics and the spread of invading organisms. *Theoretical Population Biology* 43:141–158

Lewis MA, Pacala SW. Modeling and analysis of stochastic invasion processes. *Journal of Mathematical Biology*. In press

Lubina J, Levin SA (1988). The spread of a reinvading organism: Range expansion in the Californean sea otter. *The American Naturalist* 131:526–543

Lui R (1983). Existence and stability of a non-linear integral operator. *Journal of Mathematical Biology* 16:199–220

Lui R (1989a). Biological growth and spread modeled by systems of recursions. I. Mathematical theory. *Mathematical Biosciences* 93:267–296

Lui R (1989b). Biological growth and spread modeled by systems of recursions. II. Biological theory. *Mathematical Biosciences* 93:297–312

Metz JAJ, van den Bosch F (1995). Velocities of epidemic spread. In *Epidemic Models: Their Structure and Relation to Data*, ed. Mollison D, pp. 150–186. Cambridge, UK: Cambridge University Press

Moegle H, Knorpp F, Bögel K, Arata A, Dietz N, Dietzhelm P (1974). Zur Epidemiologie der Wildtollwut. Untersuchungen im südlichen Teil der Bundesrepublik Deutschland. *Zentralblatt für Veterinär Medizin B* 21:647–59

Mollison D (1972a). Possible velocities for a simple epidemic. *Advances in Applied Probability* 4:233–257

Mollison D (1972b). The rate of spatial propagation of simple epidemics. *Proceedings of the Sixth Berkeley Symposium on Mathematical Statistics and Probability* 3:579–614

Mollison D (1977). Spatial contact models for ecological and epidemic spread. *Journal of the Royal Statistical Society B* 39:283–326

Mollison D (1991). Dependence of epidemic and population velocities on basic parameters. *Mathematical Biosciences* 107:255–287

Osae-Danso F. *Invasions of pests and diseases in Africa*, Department of Phytopathology, Wageningen. Unpublished

Radcliffe J, Rass L (1983). Wave solutions for the deterministic non-reducible N-type epidemic. *Journal of Mathematical Biology* 17:45–66

Radcliffe J, Rass L (1984a). The spatial spread and the final size of models for the deterministic host-vector epidemic. *Mathematical Biosciences* 70:123–146

Radcliffe J, Rass L (1984b). The uniqueness of wave-solutions for the deterministic non-reducible N-type epidemic. *Journal of Mathematical Biology* 19:303–308

Radcliffe J, Rass L (1984c). The spatial spread and final size of the deterministic non-reducible N-type epidemic. *Journal of Mathematical Biology* 19:309–327

Radcliffe J, Rass L (1984d). Saddle point approximations in N-type epidemics and contact-birth processes. *Rocky Mountain Journal of Mathematics* 14:599–617

Radcliffe J, Rass L (1985). The rate of spread of infection in models for the deterministic host–vector epidemic. *Mathematical Biosciences* 74:257–273

Radcliffe J, Rass L (1986). The asymptotic spread of propagation of the deterministic non-reducible N-type epidemic. *Journal of Mathematical Biology* 23:341–359

Radcliffe J, Rass L (1991). Effect of reducibility on the deterministic spread of infection in a heterogeneous population. In *Mathematical Population Dynamics: Proceedings of the Second International Conference*, ed. Arino O, Axelrod DE, Kimmel M, pp. 93–114. New York, NY, USA: Marcel Dekker

Radcliffe J, Rass L (1993). Reducible epidemics: Choosing your saddle. *Rocky Mountain Journal of Mathematics* 14:599–617

Radcliffe J, Rass L (1995a). Spatial branching and epidemic processes. In *Mathematical Population Dynamics: Analysis and Heterogeneity*, ed. Arino O, Langlais M, Kimmel M, pp. 147–170. Winnipeg, Canada: Wuertz

Radcliffe J, Rass L (1995b). Multitype contact branching processes. *Proceedings of First World Conference on Branching Processes, Springer Lecture Notes in Statistics* 99:239–179

Radcliffe J, Rass L (1996). The asymptotic behavior of a reducible system of nonlinear integral equations. *Rocky Mountain Journal of Mathematics* 26:731–752

Radcliffe J, Rass L (1997). Discrete time spatial models arising in genetics, evolutionary game theory, and branching processes. *Mathematical Biosciences* 140:101–129

Radcliffe J, Rass L (1998). Spatial mendelian games. *Mathematical Biosciences* 151:191–218

Radcliffe, J, Rass, L., *Spatial Deterministic Epidemics*. American Mathematical Society Surveys and Monographs. Book in preparation

Sherratt JA, Eagan BT, Lewis MA (1997). Oscillations and chaos behind predator–prey invasion: Mathematical artifact or ecological reality? *Philosophical Transactions of the Royal Society of London B* 352:21–38

Shigesada N, Kawasaki K, Teramoto E (1986). Traveling periodic waves in heterogeneous environments. *Theoretical Population Biology* 30:143–160

Shigesada N, Kawasaki K, Teramoto E (1987). The speed of travelling frontal waves in heterogeneous environments. In *Mathematical Topics in Population Biology, Morphogenesis and Neurosciences, Lecture Notes in Biomathematics*, Vol. 71, ed. Teramoto E, Yamaguti M, pp. 88–97. Berlin, Germany: Springer

Shigesada N, Kawasaki K, Takeda Y (1995). Modeling stratified diffusion in biological invasions. *The American Naturalist* 146:229-251

Steck F, Wandeler A (1980). The epidemiology of fox rabies in Europe. *Epidemiological Review* 2:71–96

Thieme HR (1977a). A model for the spatial spread of an epidemic. *Journal of Mathematical Biology* 4:337–351

Thieme HR (1977b). The asymptotic behaviour of solutions of nonlinear integral equations. *Math-*

ematische Zeitschrift 157:141–154

Thieme HR (1979a). Asymptotic estimates of the solutions of nonlinear integral equations and asymptotic speeds for the spread of populations. *Journal für reine und angewandte Mathematik* 306:94–121

Thieme HR (1979b). Density-dependent regulation of spatially distributed populations and their asymptotic speed of spread. *Journal of Mathematical Biology* 8:173–187

van de Lande H, Zadoks JC. Spatial patterns of spear rot in oil palm plantations in Suriname. *Plant Pathology* 48. In press

van den Bosch F, Metz JAJ, Diekmann O (1990a). The velocity of spatial population expansion. *Journal of Mathematical Biology* 28:529–565

van den Bosch F, Verhaar MA, Buiel AAM, Hoogkamer W, Zadoks JC (1990b). Focus expansion in plant disease. IV. Expansion rates in mixtures of resistant and susceptible hosts. *Phytopathology* 80:598–602

van den Bosch F, Zadoks JC, Metz JAJ (1994). Continental expansion of plant disease: A survey of some recent results. In *Predictability and Nonlinear Modelling in Natural Sciences and Economics*, ed. Grasman J, van Straten G, pp. 274–281. Dordrecht, Netherlands: Kluwer Academic Publishers

van Doorn AM (1959). Investigations on the occurrence and the control of downy mildew (*peronospora destructor*) in onions. [In Dutch with English summary.] *Tijdschrift over Plantenziekten* 65:193–255

van Kampen NG (1981). *Stochastic Processes in Physics and Chemistry.* Amsterdam, Netherlands: North-Holland

Veit RR, Lewis MA (1996). Dispersal, population growth and the Allee effect: Dynamics of the house finch invasion of North America. *The American Naturalist* 148:255–274

Weinberger HF (1978). Asymptotic behaviour of models in population genetics. In *Nonlinear Partial Differential Equations and Applications, Lecture Notes in Mathematics*, Vol. 648, ed. Chadam JM, pp. 47–98. Berlin, Germany: Springer

Weinberger HF (1982). Long-time behaviour of a class of biological models. *SIAM Journal of Mathematical Analysis* 13:353–396

Williamson EJ (1961). The distribution of larvae of randomly moving insects. *Australian Journal of Biological Sciences* 14:598–604

Zhang Y (1993). A shape theorem for epidemics and forest fires with finite range interactions. *Annals of Probability* 21:1755–1781